

GENERATION OF NANOSECOND OPTICAL PULSES WITH CONTROLLED REPETITION RATE USING IN-CAVITY INTENSITY MODULATED BRILLOUIN ERBIUM FIBER LASER

H. E. Kotb, M. Y. Shalaby, and M. H. Ahmed

Laser and Optical Communications Laboratory
Faculty of Engineering, Ain Shams University, Cairo, Egypt

Abstract—A multimode Brillouin Erbium Fiber Laser BEFL, at 1550 nm band, with in-cavity intensity modulation is demonstrated. The output of the laser is in the form of nanosecond pulses. The longitudinal mode separation is increased, which results in both reducing the number of oscillation modes and, at the same time, changing the output pulses repetition rate to be multiples of the round trip cavity frequency. It is also demonstrated that the number of modes is greatly reduced by the combination of active mode locking and the group velocity dispersion arising from the change in the refractive index at each mode due to the change in its gain within the Brillouin gain bandwidth. A case of a quasi single mode is reached where the output is nearly CW with very low sinusoidal modulation index.

1. INTRODUCTION

Generation of nanosecond light pulses is of great interest. Active mode locking is one of the techniques used to obtain such short light pulses. Brillouin fiber laser is a suitable candidate for this purpose. Stimulated Brillouin Scattering SBS is a nonlinear amplification mechanism that depends, among others, on fiber parameters and Brillouin pump BP linewidth. The gain reduces by a factor $\Delta\nu_p/\Delta\nu_B$ if pump linewidth increases where $\Delta\nu_p$ is the pump linewidth, and $\Delta\nu_B$ is the Brillouin gain bandwidth. Frequency shift between pump wave and Stokes wave in Brillouin scattering depends on the scattering angle. Frequency shift is maximum in the backward direction and zero in the forward direction. For the backward scattered wave that is of interest in optical

fibers, the maximum frequency shift is typically around 11 GHz with a scattered linewidth of about 20 MHz [1–3].

Generation of highly coherent laser light can be attained profiting from the narrow linewidth of SBS. Erbium amplification along with SBS are used to implement an Erbium Brillouin Fiber Laser [4–7]. For Dense Wavelength Division Multiplexing DWDM applications, multiwavelength Brillouin Erbium fiber laser was realized where each Stokes signal acts as a new pump to generate another Stokes signal downshifted by 11 GHz (about 0.088 nm). 24 CW channels around 1560 nm are obtained by this technique [8–10].

Active mode locking transforms the CW laser output into pulses of higher peak power and a repetition rate determined by the cavity round trip time [11]. A phase locked loop PLL can be used in active mode locking to reduce pulse timing jitter and phase noise [12]. Employing photonic crystal fiber in conjunction with a Bismuth based Erbium doped fiber, aims to reduce gain medium length [13]. As a result of the higher nonlinearity of photonic crystal fibers [14–22] and hence the lower pump power required, the generation of higher order Stokes is made easier enabling the interference between the pump wave and higher order Stokes waves to generate microwave to millimeter waves using a Brillouin laser [23]. Also the dynamics of active mode locking is analyzed to show the required time to reach steady state, the width of pulses produced, and the threshold condition for mode locking [24].

Simultaneous mode locking and Q-switching are used to obtain ultrashort pulses with energies in the mJ range [25]. SBS can play the role of Q-switching where a phase conjugating SBS reflector is employed in a Nd:YAG rod for the purpose of Q-switching and moreover to correct the beam phase distortions and hence obtain a transverse fundamental mode. Another acousto-optic modulator serves in mode locking and generate picosecond pulses.

To increase SBS efficiency in a Brillouin fiber laser, BP is tuned to a short fiber length cavity [26] which adds other features: (a) BP linewidth is filtered by the cavity which increases SBS efficiency, (b) where this filtering decreases BP power allowed to propagate inside the cavity, but the previous decrease in BP power is compensated by the accumulation of power inside the cavity at resonance. These effects have a net increase in SBS efficiency. An extra advantage is gained through stabilizing the BP frequency with the cavity using an electronic feedback circuit reducing to a large extent the BP laser frequency jitter [27].

In this paper, we demonstrate the generation of nanosecond optical pulses with a controlled repetition rate through the use of a BEFL with active mode locking. We show the possibility of obtaining

a pulse rate at multiples of the cavity round trip frequency. Moreover we demonstrate the interplay between the group velocity dispersion among the different modes and the resulting number of oscillating modes. Finally, we show that the number of oscillating modes can be greatly reduced where a case of nearly single mode is reached. In our setup, BP is not allowed to circulate in the cavity (using an in-line fiber isolator). The relatively high BP linewidth in this case (10 MHz) is compensated by the use of a long SM fiber (2.1 km). Only Stokes scattered wave is filtered by the cavity resulting in a multimode oscillation (FSR = 95.8 kHz and Brillouin linewidth is around 20 MHz). In-cavity loss modulation at $f_0 = 95.8$ kHz, the fundamental resonance frequency, lock in phase these modes and produce nanosecond pulses of pulse width equal to the reciprocal of the Brillouin linewidth. The group index variation with the modes frequency results in a great reduction in the number of oscillating modes and this is justified from our measurements of the Brillouin bandwidth in our experiment. Loss modulation, at “ n ” multiples of “ f_0 ”, decrease the number of oscillating modes by “ n ” and increase the pulse repetition rate by the same factor. A limit is reached when the intensity modulation frequency is approximately equal to half the Brillouin linewidth, a case of a nearly single mode oscillation.

2. EXPERIMENTS AND RESULTS

2.1. CW-Brillouin Laser Beam Oscillation

We show first the operation of EDFL as a CW laser source. The set-up is connected as shown in Fig. 1. A SMF (2.1 km length) is excited with optical wave BP, SBS scattering occur in the backward

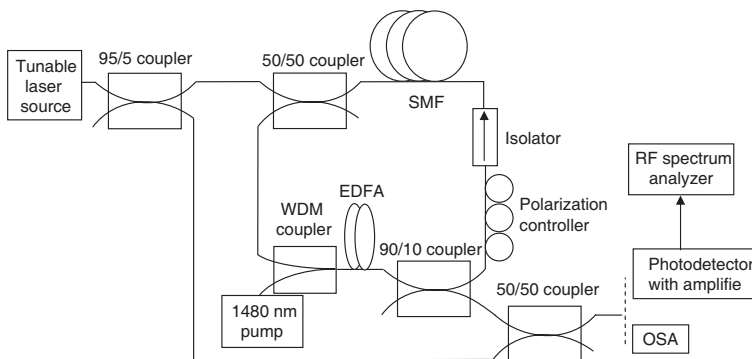


Figure 1. Experimental set-up of BEFL.

direction. Hence using an isolator as shown does not allow except SBS to propagate inside the loop which makes it the only candidate for oscillation. Since the Brillouin frequency shift is small, in order of 11 GHz in the silica fiber, we can use a pump beam in the 1550 nm C-band and an EDFA as an amplifier in the loop. As the stimulated Raman scattering SRS has a wavelength upshift of about 11 nm in silica fiber, it becomes out of the amplification range of the EDFA even if the isolator is not present.

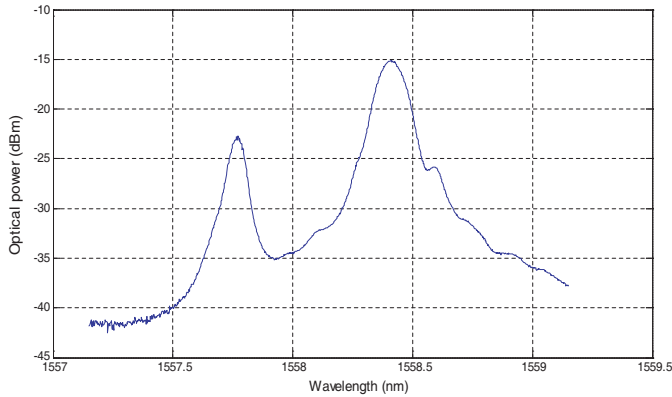


Figure 2. EDFL spectrum.

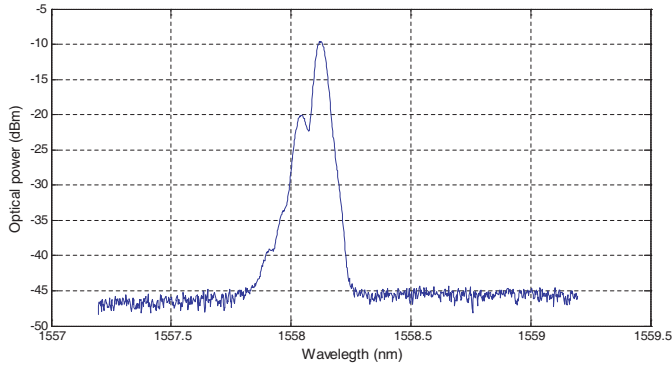


Figure 3. Mixed BEFL and BP spectrum, the BEFL peak power is at 1558.128 nm.

First, the tunable laser source is turned off; the 1480 nm pump laser source of the EDFA amplifier is turned on; and its power is set at 58 mW. Oscillations occur at random frequencies, where these oscillations frequencies are not stable and change continuously. The

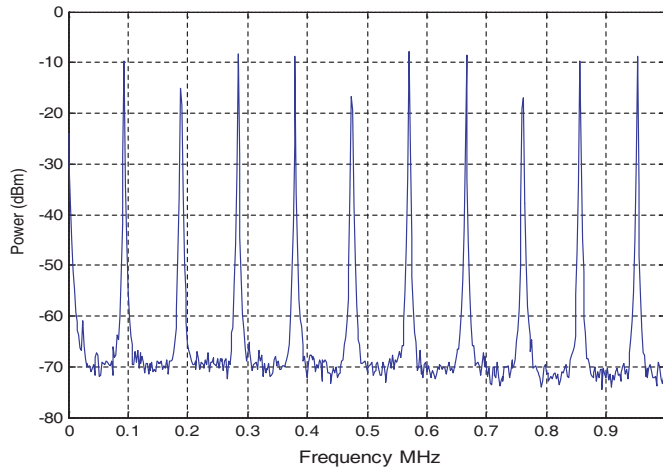


Figure 4. Beating between the multimode oscillations of BEFL displayed on the RF spectrum analyzer. The resolution bandwidth RBW is adjusted at 1 KHz.

spectrum of the optical output is displayed on the optical spectrum analyzer as shown in Fig. 2.

As seen in Fig. 2, there are two peaks resulting from the free running mode of the Erbium doped fiber laser (EDFL). These peaks are at 1557.77 and 1558.45 nm. The wavelength of the tunable laser source is adjusted to the wavelength of maximum gain in the EDFL spectrum. The optical power of the tunable laser source is set to 50 mW that acts as a Brillouin pump (BP). The power of the BP is halved due to the existence of the 3 dB coupler in the path of the BP. It is injected into the SMF in the clockwise direction and blocked by the isolator, which prevents injection locking to BP. The BP generates an additional gain in the counter-clockwise direction at a frequency shift from the BP frequency by the Stokes shift in the SMF. This frequency shift equal 11 GHz which is equivalent to 0.088 nm. The combined spectrum of BEFL and BP is shown in Fig. 3 after adjusting the tunable laser wavelength to produce the maximum power of the SBS wave.

Since the resolution of the optical spectrum analyzer is 0.05 nm (which is equivalent to 6.24 GHz around 1550 nm), the details of the spectrum of the BEFL cannot be seen in the optical spectrum analyzer. It can be analyzed using Photodetector which converts the optical signal into RF signal (Photodetector at 1.55 μm with amplifier (PDA10CF-EC), its modulation bandwidth is 150 MHz). This signal spectrum is monitored using RF spectrum analyzer which is shown in Fig. 4. It is clear that the spectrum is multimode with spectral

spacing 95.8 kHz that is equivalent to the round trip delay of the fiber loop. The beating between these modes leads to the spectrum shown in Fig. 4. This output is due to a multi-beating process which can be explained as follows.

The output at 95.8 kHz is the result of a beating at the photodetector of each mode with the mode next to it (above and below). The output at $95.8 \times 2 = 191.6$ kHz is the result of beating of each mode with the one separated from it by ± 191.6 kHz and so on. Due to the random phase relation between modes, the spectrum is not stable and randomly changes.

Changing the position of the pedals of the polarization controller creates side modes between the shown fundamental modes. This proves that the oscillation spectrum is polarization sensitive. Adjusting the pedals position will suppress, to a large extent, these side modes.

To measure the Brillouin linewidth, two Brillouin Stokes in the same direction separated by frequency shift greater than the expected Brillouin width are created. It is expected that the two BEFLs are independent from each other due to their different oscillation frequencies. This is done by applying two Brillouin pumps shifted in frequency from each other. This shift is achieved using acousto-optic modulator AOM that shifts the optical frequency by approximately 100 MHz. Generation of two Stokes shifted by 100 MHz is realized as follows: The optical signal from the tunable laser diode is split using 3-dB directional coupler, one of the two branches is connected to the AOM. The output of the AOM is connected to one of the inputs of another 3-dB directional coupler and the other input of the directional coupler is connected to a variable attenuator (adjusted at 3-dB) which is also connected to the other output of the first directional coupler (Fig. 5). This attenuator is used to balance the input power to the

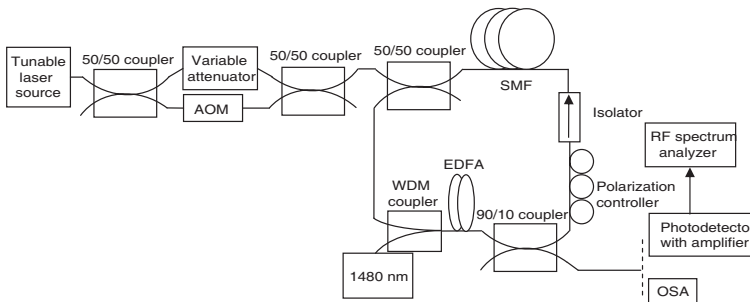


Figure 5. Schematic diagram of BEFL with two Stokes oscillations separated by 100 MHz.

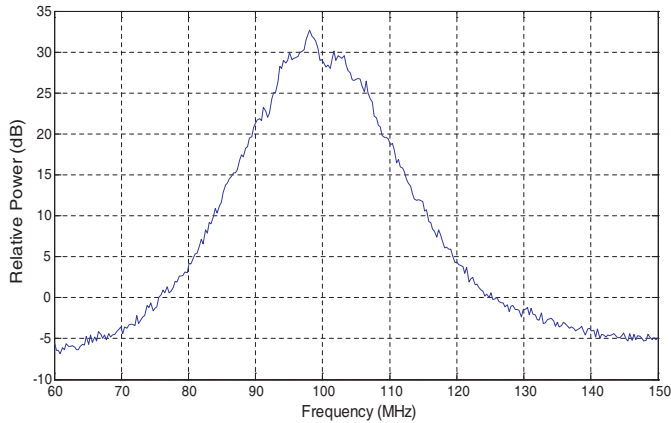


Figure 6. RF spectrum centered around the AOM shift frequency, since the RBW is 1 MHz, the envelope of BEFL modes are demonstrated.

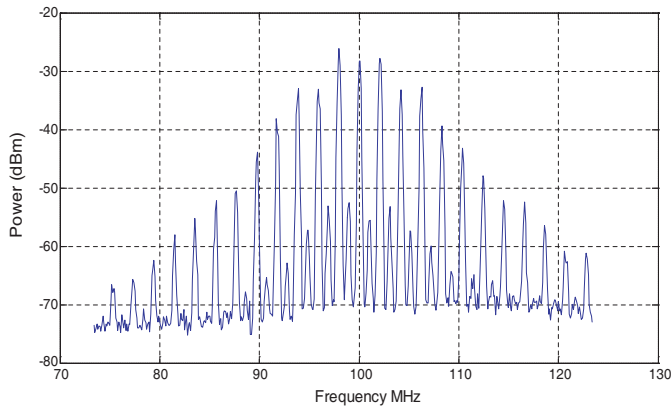


Figure 7. Mode details of the RF spectrum around the AOM shift frequency.

second directional coupler, since the AOM attenuates the signal by 3-dB so without this attenuator the two Brillouin stokes will have different powers, which will result in one signal with higher power taking more gain than the other in the EDFA. Therefore, the lower signal will be more suppressed. The frequency shift of the AOM is adjusted to 99.68 MHz by adjusting the DC voltage at its modulation input at 4 V. This setting reduces the insertion loss of the AOM to a minimum value.

After adjusting the polarization controller, a Lorentzian-like curve

is shown on the RF spectrum analyzer, since the resolution bandwidth (RBW) is 1 MHz, an envelope only without mode details is shown in Fig. 6. Reducing the RBW to 1 kHz, the mode details are clearly viewed (Fig. 7). This clarifies the multimode structure of the BEFL with mode separation equals to round trip free spectral range. This figure is obtained by averaging over (50) traces. The phase relation between these modes is not stationary in time. We notice that some frequency components have less amplitude than others. The appearance of this figure is due to the averaging process and this random phase relation. The spectral width of the curve in Fig. 6 is extracted by fitting it to a Lorentzian function, since the Brillouin gain has a Lorentzian spectrum of the form [1]

$$G_B(\omega) = \frac{g_p (\Gamma_B/2)^2}{(\omega - \omega_B)^2 + (\Gamma_B/2)^2}$$

where g_p is the peak value of the Brillouin gain at ω_B , $g_p \approx 5 \times 10^{-11}$ m/W, $\Gamma_B = \frac{1}{T_B}$ and T_B is the acoustic phonon lifetime and equal 5 ns, and the gain spectrum bandwidth is $\Delta\nu_B = \Gamma_B/2\pi$.

The spectrum measured on the RF spectrum analyzer $\Delta\nu$ around 100 MHz is the autocorrelation of the photodetected current which will give a Lorentzian spectrum of twice the width of the Brillouin spectrum; hence $\Delta\nu_B = \Delta\nu/2$. We find that Brillouin linewidth equals approximately 4.9 MHz. This smaller bandwidth than what is expected is attributed to the multibeating process used and explained before.

2.2. Mode Locking of the Brillouin Laser Beam

In this section, we demonstrate mode locking of the previously obtained multimode oscillation of the BEFL. Active mode locking of these modes will generate optical pulses with pulse width that equals the inverse of the spectral width of the Brillouin gain spectrum. Active mode locking is realized by inserting an AOM inside the cavity. The zero order output of the AOM is connected to 90/10 coupler and its electrical modulation input is connected to a wave generator adjusted to generate pulses of frequency exactly equals to the mode separation which is 95.8 kHz. The choice of the zero order output of the AOM is because it does not change the optical frequency and the AOM acts as a switch and not as a frequency shifter. The AOM switch is on when the voltage at the modulation input is zero, while the switch is off at voltage levels more than 4 V. As a result of amplitude modulation, side modes generated around the fundamental mode with frequency separation 95.8 kHz will act as the seeds of the longitudinal modes of BEFL producing mode locking. This is verified by obtaining a train of

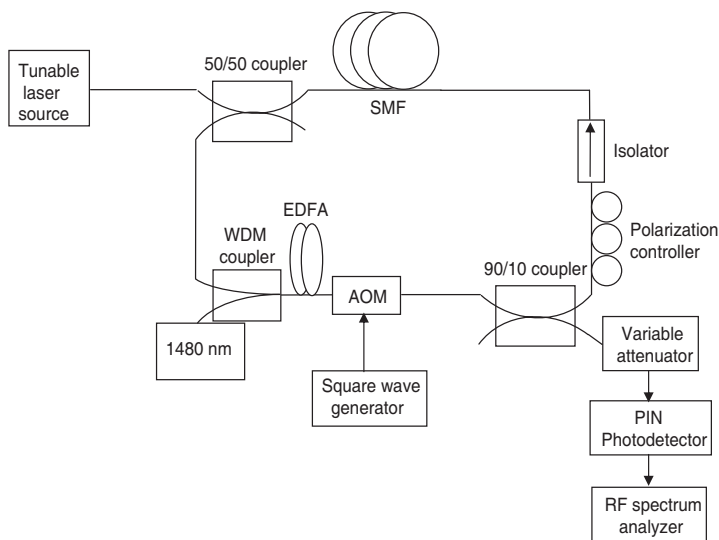


Figure 8. Schematic diagram of the set-up involving active mode locking.

pulses from the cavity output. These pulses have pulse width which is approximately equal the inverse of the Lorentzian gain spectrum.

The schematic diagram of the experimental set-up is shown in Fig. 8. PIN Photodetector with modulation bandwidth 5 GHz instead of Photodetector with TIA is used in this experiment as the output pulses have high amplitude, also a variable attenuator is placed before the Photodetector to prevent any damage to the detector.

These narrow pulses are displayed on a digitizing oscilloscope (500 MHz BW) (Fig. 9(a)) when pulses of repetition rate 95.8 kHz (period equal to 10.438 μsec and pulse width equal to 390 nsec) is applied at the modulation input of the AOM. It is clear from Fig. 9(a) that only one pulse circulates in the cavity. Zooming on one of the pulses is displayed in Fig. 9(b), showing that the pulse width is about 27 nsec. The RF spectrum of the output is shown in Fig. 9(c).

The group index at each mode frequency is given by the relation [28–30]

$$n_g = n_{g0} + \left(\frac{g_p c P_p}{\Gamma_B A_{eff}} \right) \frac{1 - \delta^2}{(1 + \delta^2)^2}$$

where P_p is the pump power and equal 50 mW, g_p is the gain coefficient $\approx 5 \times 10^{-11}$ m/W, n_{g0} is the group index at the peak of the Brillouin gain and equal 1.47, $\Gamma_B = \frac{1}{T_B}$ and T_B is the acoustic phonon lifetime

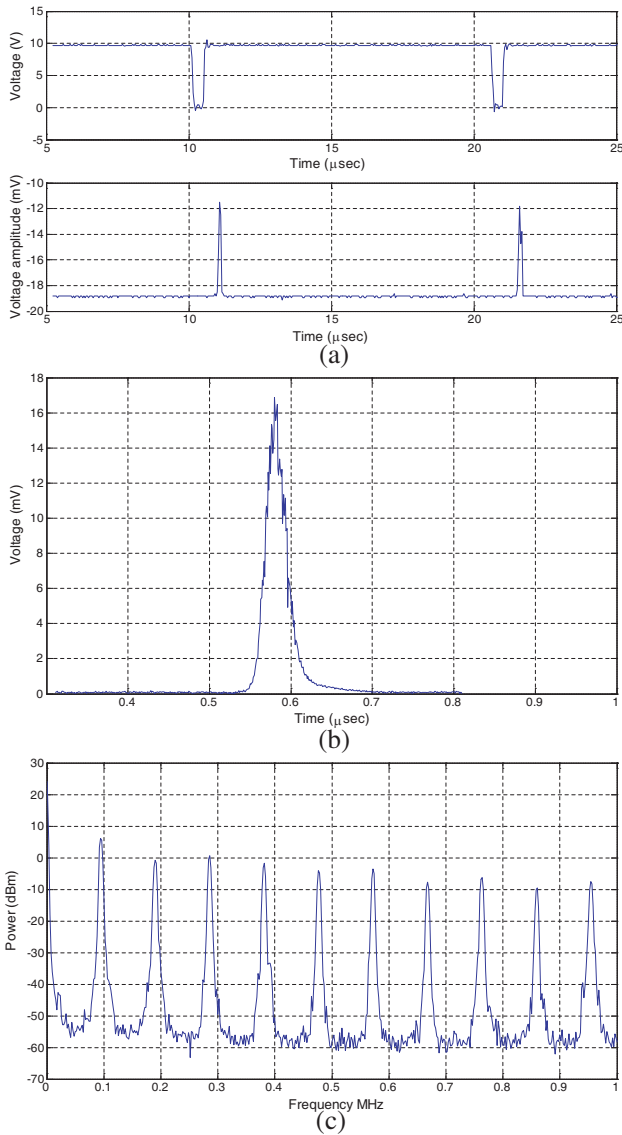
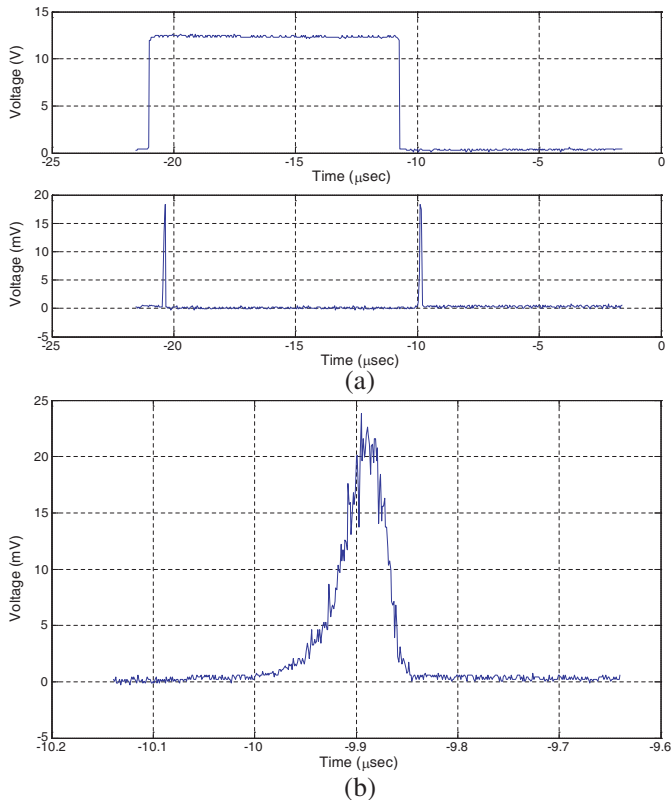


Figure 9. Mode locking effect at frequency on the modulation input of the AOM equals to 95.8 KHz, (a) train of mode locking pulses (down trace) of repetition period 10.438 μ sec resulted from amplitude modulation of the cavity (upper trace), (b) zooming in on one of the pulses to determine its pulse width, (c) the spectrum of the mode locked BEFL.

and equal 5 ns, A_{eff} is the fiber core effective area and equal $28 \mu\text{m}^2$, $\delta = 2(\Omega - \Omega_B)/\Gamma_B$ is the detuning parameter, where $\Omega_B = 2\pi\nu_B$, ν_B is the Brillouin downshift frequency equal to 11 GHz and $\Omega = \omega_p - \omega_s$ with ω_p the pump frequency and ω_s the Stokes frequency at each mode.

For the parameters in our experiment there is a considerable change in group velocity of the different modes. For the range $-1 \leq \delta \leq 1$ the refractive index changes by $\pm 5.5 \times 10^{-9}$, and the group velocity changes by 0.1704×10^8 m/s around their values at $\delta = 0$ (the center frequency of the Brillouin gain spectrum). Active mode locking should result in the selection of only those modes that can arrive at the acousto-optic modulator when it is turned on. After one round trip, the modes that should arrive at the acousto-optic modulator at the good timing have a detuning parameter given by $-0.28 \leq \delta \leq 0.28$ according to the values listed above. According to the cavity free spectral range this range of δ corresponds to 784 modes. This number



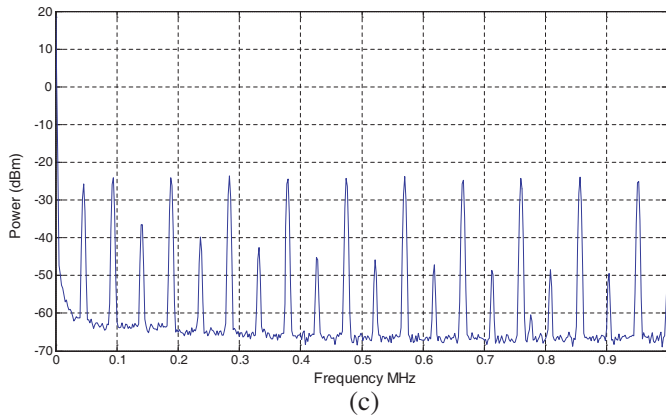


Figure 10. Mode locking effect at frequency on the modulation input of the AOM equals to 95.8 KHz, (a) train of mode locking pulses (down trace) of repetition period $10.438 \mu\text{sec}$ resulted from amplitude modulation of the cavity (upper trace), (b) zooming in on one of the pulses to determine its pulse width, (c) the spectrum of the mode locked BEFL.

decreases each round trip until a single mode operation is expected but in our experiment we discover that a number of modes are able to oscillate in the cavity which means that they propagate with the same group velocity and a form of an attraction force between these modes is behind this phenomenon. The modes of not enough power to participate in this mutual interaction propagate with their unaltered group velocity and arrive at the acousto-optic modulator at the wrong timing and hence these modes are eliminated. This explains why the measured gain bandwidth is less than what we expect of the Brillouin bandwidth in silica fibers since the number of modes that exist is much less due to this phenomenon.

The repetition rate of the pulses, connected to the AOM modulation input, is changed to 47.9 kHz (half the round trip frequency), and the pulse width is changed to $10.177 \mu\text{sec}$. Two pulses are noticed per one modulation period with pulse spacing of about $10 \mu\text{sec}$. These pulses are shown in Fig. 10(a). Due to the delay between the two electrical channels on the oscilloscope, one of the pulses appear during the high voltage and the other during the low voltage of the AOM driving signal, indeed these two pulses exist during the low voltage. Zooming on one of the two pulses is shown in Fig. 10(b). The RF spectrum of these mode locked pulses is shown in Fig. 10(c). It is clear that only one pulse circulates in the cavity (about 60 ns width), and extra-modes are generated when the original modes

create their own sidebands through intensity modulation at 47.9 kHz.

The repetition rate of the modulation pulses is now changed to 283 KHz. This frequency is approximately three times of the round trip frequency. Train of pulses is observed with the same repetition rate. Fig. 11(a) shows this train of pulses where three pulses co-circulate in the cavity. Fig. 11(b) shows the RF spectrum of these pulses. It is clear that the mode separation is 283 kHz. The explanation of these results is that the fundamental mode (the mode at the highest gain of the Brillouin spectrum) starts oscillation and then when it is intensity modulated at 283 kHz it creates sidebands separated by ± 283 kHz.

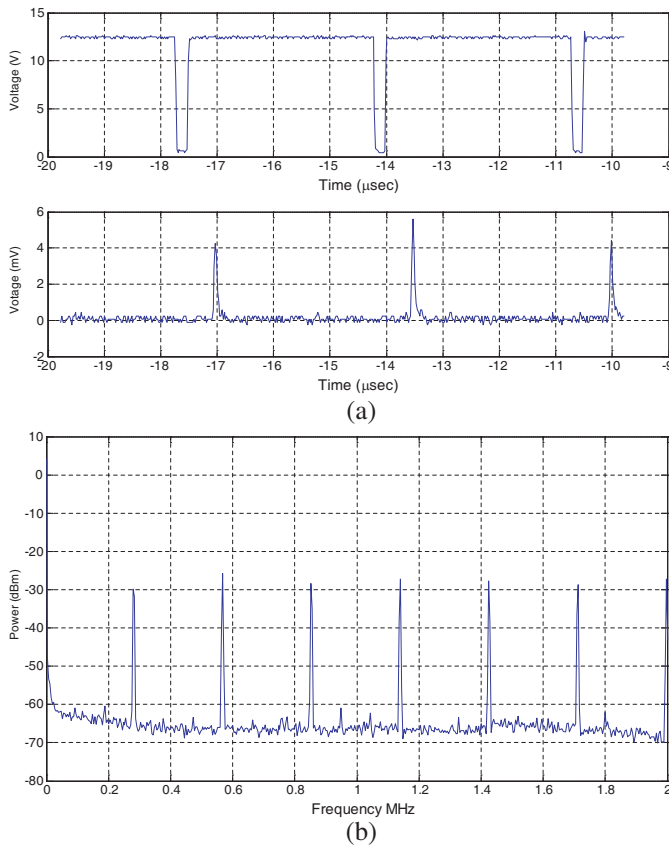


Figure 11. Mode locking effect at frequency on the modulation input of the AOM equals to 283 KHz, (a) train of mode locked pulses (down trace) of repetition $3.53 \mu\text{sec}$ resulted from amplitude modulation of the cavity (upper trace), (b) the spectrum of the pulses.

These modes continue to oscillate in the cavity and are phase locked all together. The modes separated by ± 95.8 kHz and ± 191.6 kHz from the fundamental mode have no enough gain to build up and therefore disappear.

2.3. Quasi-single Mode Brillouin Laser Operation

In the previous section, we conclude that the number of oscillating modes inside the cavity decreases as the cavity loss modulation frequency is multiples of the round trip frequency. Therefore in this section we try to decrease the number of oscillating modes to the least possible. The repetition rate of the modulation pulses is changed to 9 MHz. Very interesting result is reached, the RF spectrum resulted in two RF harmonics separated by 9 MHz with around 20 dB difference in power (Fig. 12(a)). So we can deduce that the output of the BEFL

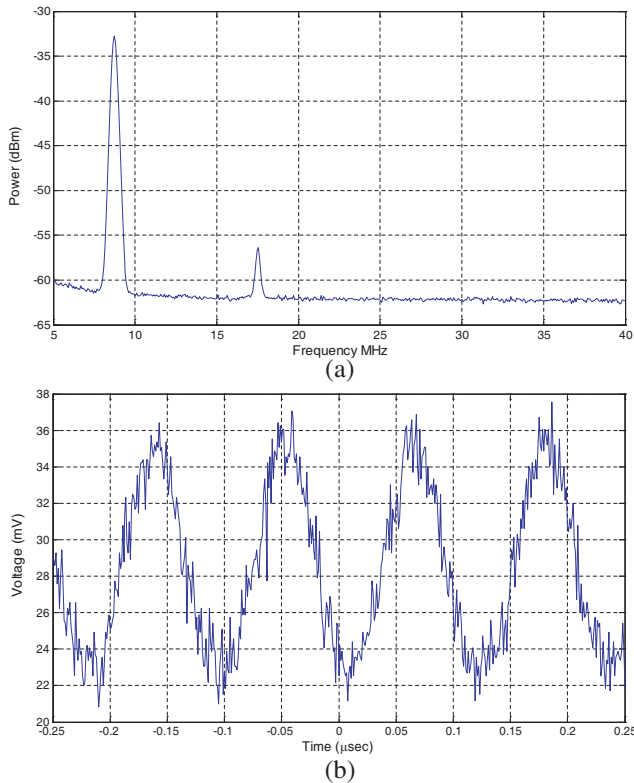


Figure 12. (a) The spectrum of the output pulses when the modulation pulses frequency is 9 MHz, (b) the output in time domain (photodetector with TIA is used to detect this signal).

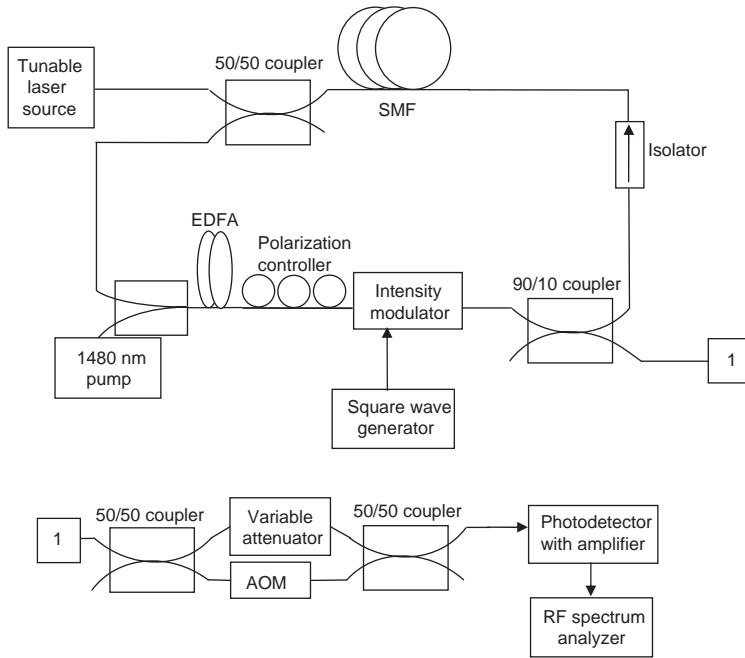


Figure 13. The experimental setup to check the single mode operation of BEFL with high modulation frequency.

is in the form of a fundamental mode and two weak side modes. This is proved in time domain by the fact that the detected signal is nearly a sinusoidal wave (Fig. 12(b)) with very small modulation index at the beating frequency between the fundamental mode and the neighboring modes shifted by 9 MHz.

An experimental set-up is used at this step to answer the postulate stating that the increase of the intensity modulation frequency of the cavity may lead to a single mode operation of the BEFL. The aim of this setup is also to check whether single mode operation is reached or not. The set-up is shown in Fig. 13. Here the acousto-optic modulator is replaced by intensity modulator since the latter has higher bandwidth which can permit us to increase the modulation frequency. However, its insertion loss is around 6 dB, which is 3 dB higher than that of the acousto-optic modulator. The polarization controller is connected before the intensity modulator as its performance is polarization dependent, so the polarization status must be controlled to have the best output. A 3-dB coupler is connected to the 90/10 coupler output; an acousto-optic modulator is connected to one of its arms; and

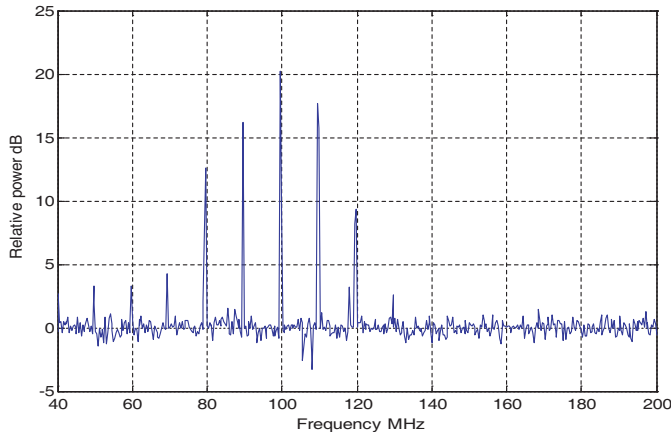


Figure 14. RF spectrum at amplitude modulation frequency 10 MHz, pulse width 40 ns and EDFA pump power 27 mW.

the output of the acousto-optic modulator is connected to one of the inputs of another 3-dB coupler. The other two arms are connected together. The acousto-optic modulator acts as a frequency shifter which shifts the optical frequency by 100 MHz. This arrangement will serve to shift the frequency spectrum around 100 MHz.

The pump power of the EDFA amplifier is adjusted to 27 mW. The spectrum measured on the spectrum analyzer is a combination of the spectrum of the detector and the beating spectrum of the BEFL ($H_{det}(f)S_v(f)$ where $H_{det}(f)$ is detector RF spectrum, and $S_v(f)$ is the beating spectrum of the BEFL). Therefore, the detector spectrum is eliminated by recording only the detector spectrum and subtracting it in dB from the above combined spectrum. Fig. 14 shows the interference spectrum at modulation frequency 10 MHz with pulse width 40 ns. It is clear from the figure the existence of around five RF harmonics in the spectrum. Due to the interference between the spectrum at zero frequency and the shifted spectrum around 100 MHz, the number of modes of the BEFL deduced in this case is three.

3. CONCLUSION

In conclusion, a multimode Brillouin Erbium Fiber laser is demonstrated. The number of oscillating modes and hence the output pulse repetition rate are controlled through the choice of the RF frequency driving an optical switch inside the laser cavity. The effect of group velocity dispersion on the number of oscillating modes is studied.

A quasi-monomode limit is reached when the intensity modulation frequency is near half the Brillouin linewidth. In a future work, the single cavity will be replaced by direct coupled cavities to control the number of oscillating modes and hence obtain a pulsed narrow linewidth laser.

REFERENCES

1. Agrawal, G. P., *Non Linear Fiber Optics*, 4th edition, Chapter 9, Elsevier, 2006.
2. Singh, S. P., R. Gangwar, and N. Singh, "Nonlinear scattering effects in optical fibers," *Progress In Electromagnetics Research*, Vol. 74, 379–405, 2007.
3. Singh, S. P. and N. Singh, "Nonlinear effects in optical fibers: origin, management and applications," *Progress In Electromagnetics Research*, Vol. 73, 249–275, 2007.
4. Cowle, G. J. and D. Yu. Stepanov, "Hybrid Brillouin/Erbium fiber laser," *Optics Letters*, Vol. 21, No. 16, 1250–1252, August 1996.
5. Harun, S. W., N. Tamchek, P. Poopalan, and H. Ahmad, "L-band Brillouin-Erbium fiber laser," *Laser Physics*, Vol. 13, No. 9, 1161–1165, 2003.
6. Abdullah, M. K., S. Shaharudin, M. A. Mahdi, and R. Endut, "A widely tunable hybrid Brillouin-Erbium fiber laser (BEFL) system," *Optics & Laser Technology*, Vol. 36, 567–570, 2004.
7. Samsuri, N. M., A. K. Zamzuri, M. H. Al-Mansoor, A. Ahmad, and M. A. Mahdi, "Brillouin-Erbium fiber laser with enhanced feedback coupling using common Erbium gain section," *Optics Express*, Vol. 16, No. 21, 16475–16480, October 2008.
8. Cowle, G. J. and D. Yu. Stepanov, "Multiple wavelength generation with brillouin Erbium fiber lasers," *IEEE Photonics Technology Letters*, Vol. 8, No. 11, 1465–1467, November 1996.
9. Abd-Rahman, M. K., M. K. Abdullah, and H. Ahmad, "Multiwavelength, bidirectional operation of twin-cavity Brillouin/Erbium fiber laser," *Optics Comm.*, Vol. 181, 135–139, July 2000.
10. Chen, D. and B. Sun, "Multiwavelength fiber optical parametric oscillator based on a highly nonlinear fiber and a Sagnac loop filter," *Progress In Electromagnetics Research*, Vol. 106, 163–176, 2010.
11. Haus, H. A., "Mode-locking of lasers," *IEEE J. Selected*

- topics in Quantum Electron.*, Vol. 6, No. 6, 1173–1185, November/December 2000.
12. Zhou, Y., “The novel active mode-locking 402.5 MHz repetition rate pico-second laser based on PLL structure,” *PIERS Proceedings*, 1557–1559, Xian, China, March 22–26, 2010.
 13. Shahi, S., S. W. Harun, K. Dimyati, and H. Ahmed, “Brillouin fiber laser with significantly reduced gain medium length operating in L-band region,” *Progress In Electromagnetics Research Letters*, Vol. 8, 143–149, 2009.
 14. Zheng, L. G. and W. X. Zhang, “Study on bandwidth of 2-D dielectric PBG material,” *Progress In Electromagnetics Research*, Vol. 41, 83–106, 2003.
 15. El-Dahshory, M. A., A. M. Attiya, and E. A. Hashish, “Design equations of two dimensional dielectric photonic bandgap structures,” *Progress In Electromagnetics Research*, Vol. 74, 319–340, 2007.
 16. Wu, J.-J., D. Chen, K.-L. Liao, T.-J. Yang, and W. L. Ouyang, “The optical properties of Bragg fiber with a fiber core of 2-dimension elliptical-hole photonic crystal structure,” *Progress In Electromagnetics Research Letters*, Vol. 10, 87–95, 2009.
 17. Rostami, A. and S. Matloub, “Band structure and dispersion properties of photonic quasicrystals,” *Progress In Electromagnetics Research M*, Vol. 9, 65–78, 2009.
 18. Li, J. M., T. L. Dong, and G. J. Shan, “Enhancement of electromagnetic force by localized fields in one dimensional photonic crystal,” *Progress In Electromagnetics Research M*, Vol. 10, 59–70, 2009.
 19. Nozhat, N. and N. Granpayeh, “Specialty fibers designed by photonic crystals,” *Progress In Electromagnetics Research*, Vol. 99, 225–244, 2009.
 20. Chen, D., M.-L. V. Tse, and H. Y. Tam, “Super-lattice structure photonic crystal fiber,” *Progress In Electromagnetics Research M*, Vol. 11, 53–64, 2010.
 21. Chau, Y.-F., C.-Y. Liu, and H.-H. Yeh, “A comparative study of high birefringence and low confinement loss photonic crystal fiber employing elliptical air holes in fiber cladding with tetragonal lattice,” *Progress In Electromagnetics Research B*, Vol. 22, 39–52, 2010.
 22. Chen, D., M.-L. V. Tse, and H. Y. Tam, “Optical properties of photonic crystal fibers with a fiber core of arrays of sub-wavelength circular air holes: Birefringence and dispersion,” *Progress In*

- Electromagnetics Research*, Vol. 105, 193–212, 2010.
23. Shen, G. F., X. M. Zhang, H. Chi, and X. F. Jin, “Microwave/millimeter-wave generation using multiwavelength photonic crystal fiber Brillouin laser,” *Progress In Electromagnetics Research*, Vol. 80, 307–320, 2008.
 24. Reddy, K. P. J. and J. A. Tatum, “Dynamics of active modelocking in broad-band continuous wave lasers,” *IEEE J. of Quantum Electronics*, Vol. 29, No. 5, 1407, May 1993.
 25. Kappe, P., M. Ostermeyer, and R. Menzel, “Active modelocking of a phase conjugating SBS laser oscillator,” *Appl. Phys. B*, Vol. 80, 49–54, 2005.
 26. Zarinetchi, F., S. P. Smith, and S. Ezekiel, “Stimulated Brillouin fiber optic gyroscope,” *Optics Letters*, Vol. 16, No. 4, 229–231, February 1991.
 27. Black, E. D., “An introduction to Pound-Drever-Hall laser frequency stabilization,” *Am. J. Phys.*, Vol. 69, No. 1, 79–87, January 2001.
 28. Song, K. Y., M. G. Herraiez, and L. Thevenaz, “Observation of pulse delaying and advancement in optical fibers using stimulated Brillouin scattering,” *Optics Express*, Vol. 13, No. 1, 82–88, January 2005.
 29. Okawachi, Y., M. S. Bigelow, J. E. Sharping, Z. Zhu, A. Schweinsberg, D. J. Gauthier, R. W. Boyd, and A. L. Gaeta, “Tunable all-optical delays via Brillouin slow light in an optical fiber,” *Phys. Rev. Lett.*, Vol. 94, 153902, April 2005.
 30. Pandey, G. N., K. B. Thapa, S. K. Srivastava, and S. P. Ojha, “Band structures and abnormal behavior of one dimensional photonic crystals containing negative index materials,” *Progress In Electromagnetics Research M*, Vol. 2, 15–36, 2008.